

Synthesis, crystal structure and thermal properties of poly[bis[μ -3-(aminomethyl)pyridine- κ^2 N:N']bis-(thiocyanato- κ N)manganese(II)]

Christoph Krebs,* Inke Jess and Christian Näther

Institut für Anorganische Chemie, Christian-Albrechts-Universität zu Kiel, Max-Eyth-Str. 2, D-24118 Kiel, Germany.

*Correspondence e-mail: ckrebs@ac.uni-kiel.de

Received 11 June 2021

Accepted 28 June 2021

Edited by M. Weil, Vienna University of Technology, Austria

Keywords: crystal structure; layered structure; thermal properties; manganese thiocyanate; 3-(aminomethyl)pyridine; isotypism.

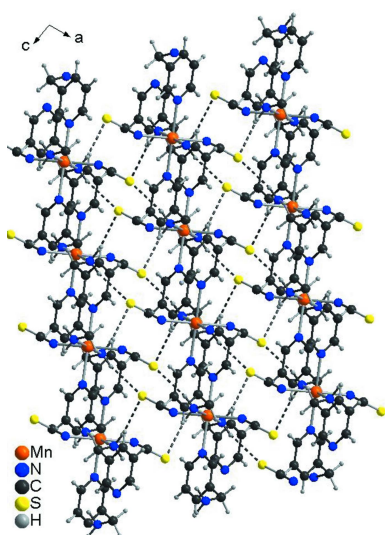
CCDC reference: 2092830

Supporting information: this article has supporting information at journals.iucr.org/e

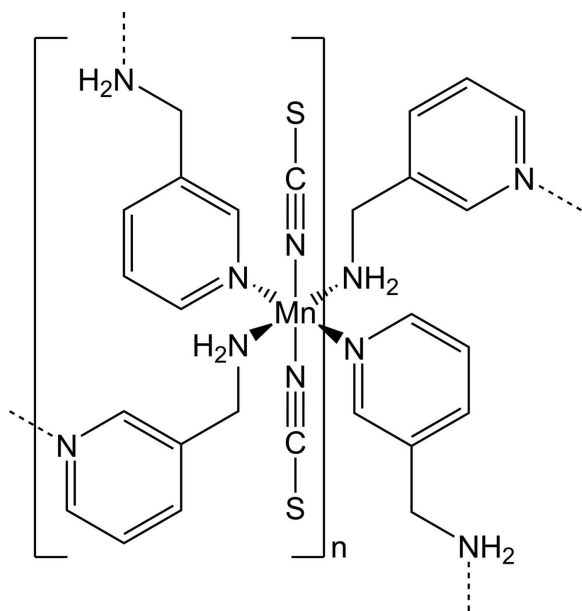
The reaction of $\text{Mn}(\text{NCS})_2$ with a stoichiometric amount of 3-(aminomethyl)pyridine in ethanol led to the formation of the title compound, $[\text{Mn}(\text{NCS})_2(\text{C}_6\text{H}_8\text{N}_2)_2]_n$, which is isotypic to its Zn, Co and Cd analogues. The manganese cation is located on a centre of inversion and is octahedrally coordinated in an all-*trans* configuration by two terminal N-bonded thiocyanate anions as well as four 3-(aminomethyl)pyridine co-ligands, of which two coordinate with the pyridine N atom and two with the amino N atom. The 3-(aminomethyl)pyridine co-ligands connect the Mn^{II} cations into layers extending parallel to $(10\bar{1})$. These layers are further connected into a three-dimensional network by relatively strong intermolecular N—H \cdots S hydrogen bonding. Comparison of the experimental X-ray powder diffraction pattern with the calculated pattern on the basis of single-crystal data proves the formation of a pure crystalline phase. IR measurements showed the CN stretching vibration of the thiocyanate anions at 2067 cm^{-1} , which is in agreement with the presence of terminally N-bonded anionic ligands. TG–DTA measurements revealed that the title compound decomposes at about 500 K.

1. Chemical context

In contrast to other small-sized ligands such as azide or cyanide anions, thiocyanate anions show many more coordination modes. Therefore, a variety of structures including discrete complexes (Prananto *et al.*, 2017; Małeck *et al.*, 2011; Wöhlert *et al.*, 2014), dimers (Mautner *et al.*, 2015; Wei & Luo, 2010; Jochim *et al.*, 2018), chains (Mautner *et al.*, 2018; Rams *et al.*, 2020), layers (Suckert *et al.*, 2016, 2017) or in very rare cases three-dimensional networks (Suckert *et al.*, 2017) can be observed. This structural variability is further enhanced by isomerism, because for an octahedral coordination with three pairs of identical ligands, five different isomers exist, including the all-*trans*, all-*cis* and three different *cis-cis-trans* configurations. These features are found in compounds with structures where the metal cations are linked by pairs of anionic ligands into chains. The majority of compounds with μ -1,3-bridging thiocyanate anions shows this behaviour. Depending on the actual metal coordination (all-*trans* or *cis-cis-trans*), linear or corrugated chains are observed (Jin *et al.*, 2007; Rams *et al.*, 2017; Böhme *et al.*, 2020; Jochim *et al.*, 2020). Moreover, even for compounds with layered thiocyanate structures, different networks are realized, in which the metal cations are linked exclusively by single anionic ligands or by both singly and doubly μ -1,3-bridging thiocyanate anions. For less chalcophilic metal cations like Mn^{II} , Fe^{II} , Co^{II} or Ni^{II} , the majority



of compounds consist of structures with only terminally N-bonding thiocyanate anions, because in this case this coordination is energetically favoured. With only mono-coordinating ligands this usually leads to the formation of discrete metal complexes with an octahedral coordination. If bridging co-ligands are used, chain structures can be realized and networks of higher dimensionality are available if additional μ -1,3-bridging thiocyanate anions are present.



Thiocyanate coordination polymers are of interest not only because of their variable structural behaviour, but also because this ligand is able to mediate reasonable magnetic exchange. We and other groups have reported many new compounds in which the metal cations are linked by μ -1,3-bridging thiocyanate anions into chains or layers (Werner *et al.*, 2015; Bassey *et al.*, 2020; Mekuimemba *et al.*, 2018; Palion-Gazda *et al.*, 2015; Neumann *et al.*, 2019; Mousavi *et al.*, 2020). In this context, we became interested in 3-(aminomethyl)pyridine, because this ligand is able to link metal cations *via* the pyridine and the amino N atom. Surprisingly, with Co^{II} we always obtained only one crystalline phase in which the Co^{II} cations are coordinated by only terminally N-bonding thiocyanate anions but linked into layers by the 3-(aminomethyl)pyridine co-ligands (Krebs *et al.*, 2021). In contrast to the Co^{II} cation, the Mn^{II} cation is more chalcophilic and usually behaves like Cd^{II} , for which compounds with μ -1,3-bridging thiocyanate anions are much easier to obtain. Therefore, we used $\text{Mn}(\text{NCS})_2$ in the present study. However, irrespective of the ratio between $\text{Mn}(\text{NCS})_2$ and 3-(aminomethyl)pyridine, we always obtained only one crystalline phase with composition $\text{Mn}(\text{NCS})_2(\text{C}_6\text{H}_8\text{N}_2)_2$. Single-crystal structure analysis revealed isotypism with the Co^{II} analogue reported recently (Krebs *et al.* 2021). Comparison of the experimental X-ray powder diffraction pattern with the calculated pattern based on single-crystal data proved that a pure crystalline phase was obtained (see Fig. S1 in the supporting information); IR investigations revealed that the CN stretching vibration is observed at 2067 cm^{-1} , in agreement with the presence of only

Table 1
Selected geometric parameters (\AA , $^\circ$).

Mn1–N1	2.1955 (15)	Mn1–N11	2.3154 (14)
Mn1–N12 ⁱ	2.2901 (14)		
N1–Mn1–N1 ⁱⁱ	180.0	N1 ⁱⁱ –Mn1–N11	90.82 (5)
N1–Mn1–N12 ⁱ	91.17 (6)	N12 ⁱ –Mn1–N11	89.52 (5)
N1–Mn1–N12 ⁱⁱⁱ	88.83 (6)	N12 ⁱⁱⁱ –Mn1–N11	90.48 (5)
N1–Mn1–N11	89.18 (5)	N1–Mn1–N11 ⁱⁱ	90.82 (5)

Symmetry codes: (i) $x - \frac{1}{2}, -y + \frac{3}{2}, z - \frac{1}{2}$; (ii) $-x, -y + 1, -z$; (iii) $-x + \frac{1}{2}, y - \frac{1}{2}, -z + \frac{1}{2}$.

terminally N-bound thiocyanate anions (Fig. S2). TG-DTA measurements showed decomposition of the compound at about 500 K, which is accompanied by an endothermic event in the DTA curve (Fig. S3). The first decomposition step might be associated with the removal of the 3-(aminomethyl)pyridine co-ligand. On further heating, an exothermic signal is observed, which indicates the decomposition of the co-ligand.

2. Structural commentary

$\text{Mn}(\text{NCS})_2(\text{C}_6\text{H}_8\text{N}_2)_2$ is isotypic with its recently reported Cd^{II} , Zn^{II} and Co^{II} analogues (Neumann *et al.*, 2017; Krebs *et al.*, 2021). The asymmetric unit consists of one Mn^{II} cation that is located on a centre of inversion as well as one 3-(aminomethyl)pyridine co-ligand and one thiocyanate anion (Fig. 1). The Mn^{II} cation is octahedrally coordinated by the N atoms of four symmetry-equivalent 3-(aminomethyl)pyridine co-ligands and two symmetry-equivalent thiocyanate anions. Two of these co-ligands coordinate through the pyridine N atom whereas the other two coordinate with the amino N atom. Each pair of identical donor atoms is in a *trans*-position (Fig. 1). The Mn–N bond length to the negatively charged thiocyanate N atom is significantly shorter than that to the

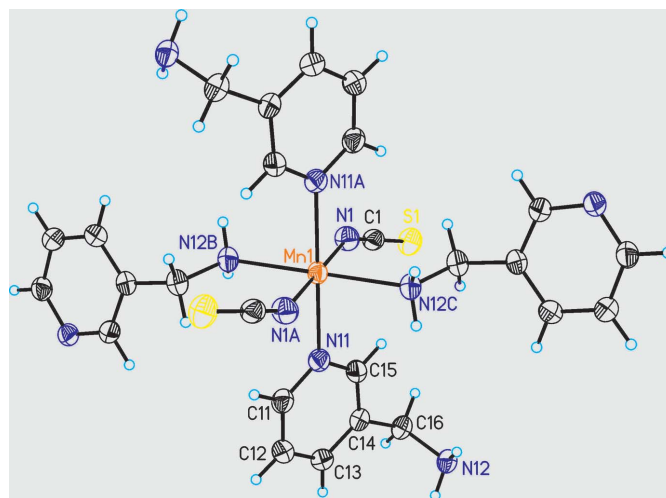


Figure 1
The coordination of the Mn^{II} cation in the title compound with displacement ellipsoids drawn at the 50% probability level. [Symmetry codes: (A) $-x, -y + 1, -z$, (B) $\frac{1}{2} - x, -\frac{1}{2} + y, \frac{1}{2} - z$, (C) $-\frac{1}{2} + x, \frac{3}{2} - y, -\frac{1}{2} + z$.]

Table 2
Hydrogen-bond geometry (Å, °).

$D-H\cdots A$	$D-H$	$H\cdots A$	$D\cdots A$	$D-H\cdots A$
$C12-H12\cdots S1^{iii}$	0.95	2.99	3.7264 (19)	136
$N12-H12A\cdots S1^{iv}$	0.91	2.81	3.7016 (16)	166
$N12-H12B\cdots S1^v$	0.91	2.66	3.5224 (15)	159

Symmetry codes: (iii) $-x + \frac{1}{2}, y - \frac{1}{2}, -z + \frac{1}{2}$; (iv) $x, y, z + 1$; (v) $x - \frac{1}{2}, -y + \frac{3}{2}, z + \frac{1}{2}$.

3-(aminomethyl)pyridine co-ligand; the Mn–N bond length to the pyridine N atom is significantly longer than that to the amino N atom of the 3-(aminomethyl)pyridine ligand (Table 1). As expected, all Mn–N bond lengths are significantly longer and shorter, respectively, compared to the Co^{II} and Cd^{II} analogues. The bond angles around Mn^{II} indicate a considerable distortion (Table 1). This is also indicated by the mean octahedral quadratic elongation of 1.0013 and the octahedral angle variance of 0.8258 (Robinson *et al.*, 1971). The Mn^{II} cations are connected by bridging 3-(aminomethyl)pyridine ligands into chains, which are further linked into layers extending parallel to (10 $\bar{1}$) by additional co-ligands (Fig. 2).

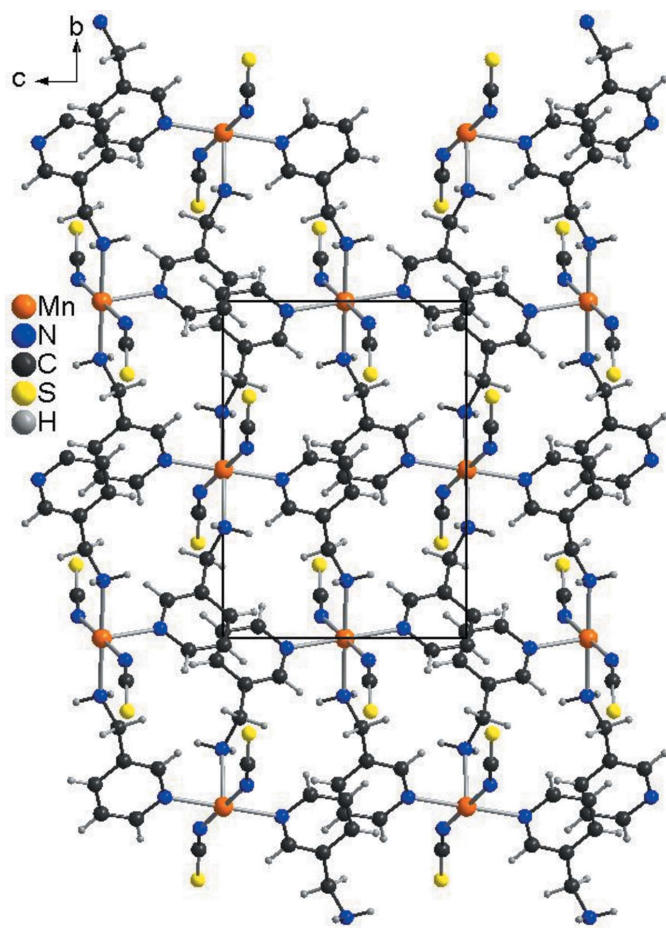


Figure 2
Crystal structure of the title compound in a view of a layer along the crystallographic a axis.

3. Supramolecular features

The layers are linked into a three-dimensional network by intermolecular N–H \cdots S hydrogen bonds between the amino H atoms and the thiocyanate S atoms (Fig. 3, Table 2). The N–H \cdots S angles indicate a relatively strong interaction and the thiocyanate S atom acts as an acceptor for two of these hydrogen bonds. There is also a C–H \cdots S interaction but the bonding angle is far from linearity, which points to a weak interaction (Table 2).

4. Database survey

In the Cambridge Structure Database (CSD, version 5.42, last update November 2020; Groom *et al.*, 2016) no Mn–3-(aminomethyl)pyridine compounds are reported but a few compounds based on Zn(NCS)₂ and Cd(NCS)₂ have been deposited. In all of the corresponding structures, the metal cations are octahedrally coordinated. This includes $M(NCS)_2[3-(aminomethyl)pyridine]_2$ ($M = Cd, Zn$; Neumann *et al.*, 2017; refcodes: QEKZEO and QEKYUD), which are isotopic to the title compound, as well as $M(NCS)_2[3-(aminomethyl)pyridine]$ ($M = Cd, Zn$; Neumann, *et al.* 2017;

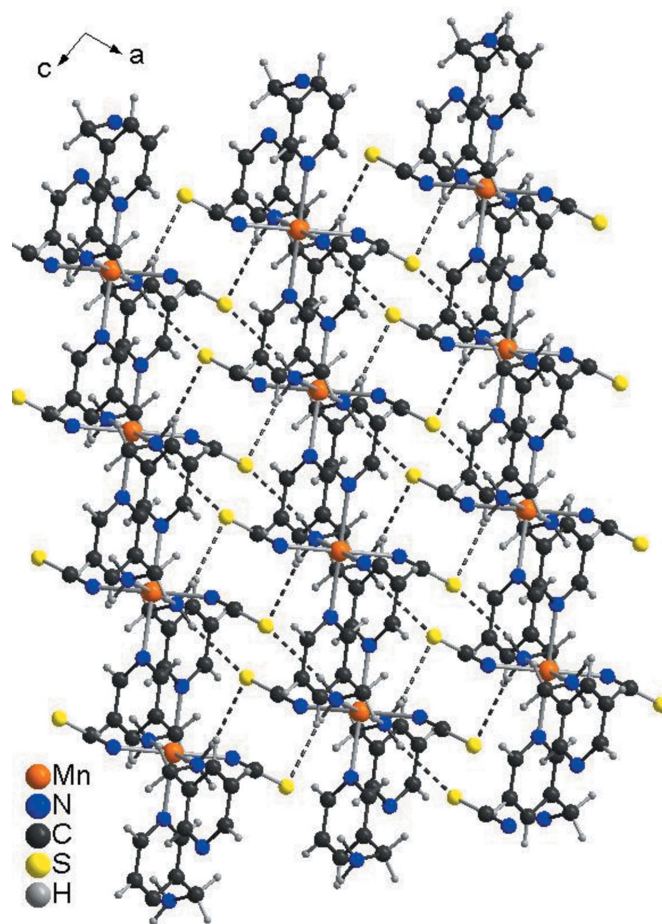


Figure 3
Crystal structure of the title compound in a view along the crystallographic b axis. Intermolecular N–H \cdots S hydrogen bonds are shown as dashed lines.

Table 3
Experimental details.

Crystal data	
Chemical formula	[Mn(NCS) ₂ (C ₆ H ₈ N ₂ S) ₂]
<i>M_r</i>	387.39
Crystal system, space group	Monoclinic, <i>P</i> 2 ₁ / <i>n</i>
Temperature (K)	200
<i>a</i> , <i>b</i> , <i>c</i> (Å)	8.2157 (3), 12.2356 (5), 8.9601 (3)
β (°)	99.736 (3)
<i>V</i> (Å ³)	887.73 (6)
<i>Z</i>	2
Radiation type	Mo <i>K</i> α
μ (mm ⁻¹)	0.99
Crystal size (mm)	0.03 × 0.03 × 0.01
Data collection	
Diffractometer	Stoe <i>IPDS2</i>
Absorption correction	Numerical (<i>X-SHAPE</i> and <i>X-RED</i> 32; Stoe, 2002)
<i>T</i> _{min} , <i>T</i> _{max}	0.856, 0.980
No. of measured, independent and observed [<i>I</i> > 2σ(<i>I</i>)] reflections	12559, 1939, 1755
<i>R</i> _{int}	0.040
(sin θ/λ) _{max} (Å ⁻¹)	0.639
Refinement	
<i>R</i> [<i>F</i> ² > 2σ(<i>F</i> ²)], <i>wR</i> (<i>F</i> ²), <i>S</i>	0.031, 0.073, 1.14
No. of reflections	1939
No. of parameters	106
H-atom treatment	H-atom parameters constrained
Δρ _{max} , Δρ _{min} (e Å ⁻³)	0.27, -0.22

Computer programs: *X-AREA* (Stoe, 2002), *SHELXS97* (Sheldrick, 2008), *SHELXL2016/6* (Sheldrick, 2015), *DIAMOND* (Brandenburg & Putz, 1999) and *PUBLICIF* (Westrip, 2010).

refcodes: QEKZIS and QEKZAK). In the latter Zn^{II} compound, dimers are observed in which two Zn^{II} cations are connected by two 3-(aminomethyl)pyridine ligands. In the Cd^{II} compound, the metal cations are linked by μ-1,3-bridging thiocyanate anions into chains that are connected into layers by the 3-(aminomethyl)pyridine ligands. This compound is the only one that contains μ-1,3-bridging thiocyanate anions and which shows a *cis-cis-trans* coordination of the metal cations. There is also one solvate with the composition Cd(NCS)₂[3-(aminomethyl)pyridine]₂-tris[3-(aminomethyl)pyridine] reported in the CSD (refcode: QEKYOX; Neumann *et al.*, 2017). Finally, Co(NCS)₂(3-(aminomethyl)pyridine)₂, which is isotopic to the title compound, is also reported (Krebs *et al.*, 2021).

5. Synthesis and crystallization

Synthesis

Mn(NCS)₂ and 3-(aminomethyl)pyridine were purchased from Alfa Aesar and all chemicals were used without further purification. Single crystals were obtained by reacting 1 mmol of Mn(NCS)₂ (175.1 mg) with 1 mmol of 3-(aminomethyl)pyridine (108.1 mg) in 4 ml of ethanol. After approximately one week, light-brown crystals were obtained, which were suitable for single crystal X-ray analysis. For the synthesis of crystalline powders, the same amounts of reactants were stirred in 2 ml of ethanol for 1 d and the precipitate was filtered off and dried in air.

Elemental analysis calculated for C₁₄H₁₆N₆MnS₂: C 43.41%, H 4.16%, N 21.69%, S 16.55%; found: C 43.32%, H 4.11%, N 21.56%, S 16.31%. IR: ν = 2971 (*m*), 2941 (*w*), 2928 (*w*), 2887 (*s*), 2875 (*w*), 2067 (*s*), 2023 (*m*), 1962(*vw*), 1861 (*vw*), 1595 (*m*), 1583 (*w*), 1480 (*m*), 1447 (*m*), 1426 (*m*), 1379 (*w*), 1361 (*w*), 1332 (*w*), 1274 (*w*), 1244 (*w*), 1229 (*w*), 1189 (*m*), 1148 (*w*), 1124 (*m*), 1089 (*m*), 1048 (*vs*), 984 (*s*), 961 (*m*), 943 (*w*), 931 (*m*), 879 (*m*), 846 (*w*), 824 (*w*), 802 (*m*), 783 (*m*), 712 (*s*), 645 (*s*), 620 (*m*), 539 (*s*) cm⁻¹.

Experimental details

The elemental analysis was performed using a EURO EA elemental analyzer fabricated by EURO VECTOR Instruments. The IR spectrum was measured using an ATI Mattson Genesis Series FTIR spectrometer, control software: *WINFIRST*, from ATI Mattson. The PXRD measurement was performed with Cu *K*α₁ radiation (λ = 1.540598 Å) using a Stoe Transmission Powder Diffraction System (STADI P) that is equipped with a MYTHEN 1K detector and a Johansson-type Ge(111) monochromator. Thermogravimetry and differential thermoanalysis (TG-DTA) measurements were performed in a dynamic nitrogen atmosphere in Al₂O₃ crucibles using a STA-PT 1000 thermobalance from Linseis. The instrument was calibrated using standard reference materials.

6. Refinement

Crystal data, data collection and structure refinement details are summarized in Table 3. All H atoms were located in a difference-Fourier map but were positioned with idealized geometry (N–H = 0.91 Å, C–H = 0.95–0.99 Å) and were refined in a riding model with *U*_{iso}(H) = 1.2*U*_{eq}(C) or 1.5*U*_{eq}(C) for amino H atoms.

Funding information

This project was supported by the State of Schleswig-Holstein and the Deutsche Forschungsgemeinschaft (grant No. NA720/5-2).

References

- Bassey, E. N., Paddison, J. A. M., Keyzer, E. N., Lee, J., Manuel, P., da Silva, I., Dutton, S. E., Grey, C. P. & Cliffe, M. J. (2020). *Inorg. Chem.* **59**, 11627–11639.
- Böhme, M., Jochim, A., Rams, M., Lohmiller, T., Suckert, S., Schnegg, A., Plass, W. & Näther, C. (2020). *Inorg. Chem.* **59**, 5325–5338.
- Brandenburg, K. & Putz, H. (1999). *DIAMOND*. Crystal Impact GbR, Bonn, Germany.
- Groom, C. R., Bruno, I. J., Lightfoot, M. P. & Ward, S. C. (2016). *Acta Cryst.* **B72**, 171–179.
- Jin, Y., Che, Y. X. & Zheng, J. M. (2007). *J. Coord. Chem.* **60**, 2067–2074.
- Jochim, A., Lohmiller, T., Rams, M., Böhme, M., Ceglarska, M., Schnegg, A., Plass, W. & Näther, C. (2020). *Inorg. Chem.* **59**, 8971–8982.
- Jochim, A., Rams, M., Neumann, T., Wellm, C., Reinsch, H., Wójtowicz, G. M. & Näther, C. (2018). *Eur. J. Inorg. Chem.* pp. 4779–4789.
- Krebs, C., Jess, I. & Näther, C. (2021). *Acta Cryst.* **E77**, 428–432.

- Małecki, J. G., Machura, B., Świtlicka, A., Groń, T. & Bałanda, M. (2011). *Polyhedron*, **30**, 746–753.
- Mautner, F. A., Scherzer, M., Berger, C., Fischer, R. C., Vicente, R. & Massoud, S. S. (2015). *Polyhedron*, **85**, 20–26.
- Mautner, F. A., Traber, M., Fischer, R. C., Torvisco, A., Reichmann, K., Speed, S., Vicente, R. & Massoud, S. S. (2018). *Polyhedron*, **154**, 436–442.
- Mekuimemba, C. D., Conan, F., Mota, A. J., Palacios, M. A., Colacio, E. & Triki, S. (2018). *Inorg. Chem.* **57**, 2184–2192.
- Mousavi, M., Duhayon, C., Bretosh, K., Béreau, V. & Sutter, J. P. (2020). *Inorg. Chem.* **59**, 7603–7613.
- Neumann, T., Germann, L. S., Moudrakovski, I., Dinnebier, R. E., dos Santos Cunha, C., Terraschke, H. & Näther, C. (2017). *Z. Anorg. Allg. Chem.* **643**, 1904–1912.
- Neumann, T., Rams, M., Tomkowicz, Z., Jess, I. & Näther, C. (2019). *Chem. Commun.* **55**, 2652–2655.
- Palion-Gazda, J., Machura, B., Lloret, F. & Julve, M. (2015). *Cryst. Growth Des.* **15**, 2380–2388.
- Prananto, Y. P., Urbatsch, A., Moubaraki, B., Murray, K. S., Turner, D. R., Deacon, G. B. & Batten, S. R. (2017). *Aust. J. Chem.* **70**, 516–528.
- Rams, M., Jochim, A., Böhme, M., Lohmiller, T., Ceglarska, M., Rams, M. M., Schnegg, A., Plass, W. & Näther, C. (2020). *Chem. Eur. J.* **26**, 2837–2851.
- Rams, M., Tomkowicz, Z., Böhme, M., Plass, W., Suckert, S., Werner, J., Jess, I. & Näther, C. (2017). *Phys. Chem. Chem. Phys.* **19**, 3232–3243.
- Robinson, K., Gibbs, G. V. & Ribbe, P. H. (1971). *Science*, **172**, 567–570.
- Sheldrick, G. M. (2008). *Acta Cryst.* **A64**, 112–122.
- Sheldrick, G. M. (2015). *Acta Cryst.* **C71**, 3–8.
- Stoe (2002). *X-Area and X-RED32*. Stoe & Cie, Darmstadt, Germany.
- Suckert, S., Rams, M., Böhme, M., Germann, L. S., Dinnebier, R. E., Plass, W., Werner, J. & Näther, C. (2016). *Dalton Trans.* **45**, 18190–18201.
- Suckert, S., Rams, M., Germann, L. S., Cegielka, D. M., Dinnebier, R. E. & Näther, C. (2017). *Cryst. Growth Des.* **17**, 3997–4005.
- Wei, R. & Luo, F. (2010). *J. Coord. Chem.* **63**, 610–616.
- Werner, S., Tomkowicz, Z., Rams, M., Ebbinghaus, S. G., Neumann, T. & Näther, C. (2015). *Dalton Trans.* **44**, 14149–14158.
- Westrip, S. P. (2010). *J. Appl. Cryst.* **43**, 920–925.
- Wöhlert, S., Runčevski, T., Dinnebier, R. E., Ebbinghaus, S. G. & Näther, C. (2014). *Cryst. Growth Des.* **14**, 1902–1913.

supporting information

Acta Cryst. (2021). E77, 765-769 [https://doi.org/10.1107/S2056989021006733]

Synthesis, crystal structure and thermal properties of poly[bis[μ -3-(aminomethyl)pyridine- κ^2 N:N']bis(thiocyanato- κ N)manganese(II)]

Christoph Krebs, Inke Jess and Christian Näther

Computing details

Data collection: *X-AREA* (Stoe, 2002); cell refinement: *X-AREA* (Stoe, 2002); data reduction: *X-AREA* (Stoe, 2002); program(s) used to solve structure: *SHELXS97* (Sheldrick, 2008); program(s) used to refine structure: *SHELXL2016/6* (Sheldrick, 2015); molecular graphics: *DIAMOND* (Brandenburg & Putz, 1999); software used to prepare material for publication: *publCIF* (Westrip, 2010).

Poly[bis[μ -3-(aminomethyl)pyridine- κ^2 N:N']bis(thiocyanato- κ N)manganese(II)]

Crystal data

[Mn(NCS)₂(C₆H₈N₂S)₂]

$M_r = 387.39$

Monoclinic, $P2_1/n$

$a = 8.2157$ (3) Å

$b = 12.2356$ (5) Å

$c = 8.9601$ (3) Å

$\beta = 99.736$ (3)°

$V = 887.73$ (6) Å³

$Z = 2$

$F(000) = 398$

$D_x = 1.449$ Mg m⁻³

Mo $K\alpha$ radiation, $\lambda = 0.71073$ Å

Cell parameters from 12559 reflections

$\theta = 2.8$ – 27.0 °

$\mu = 0.99$ mm⁻¹

$T = 200$ K

Block, light-brown

$0.03 \times 0.03 \times 0.01$ mm

Data collection

Stoe IPDS-2
diffractometer

ω scans

Absorption correction: numerical
(X-Shape and X-Red 32; Stoe, 2002)

$T_{\min} = 0.856$, $T_{\max} = 0.980$

12559 measured reflections

1939 independent reflections

1755 reflections with $I > 2\sigma(I)$

$R_{\text{int}} = 0.040$

$\theta_{\max} = 27.0$ °, $\theta_{\min} = 2.9$ °

$h = -10 \rightarrow 10$

$k = -15 \rightarrow 15$

$l = -11 \rightarrow 11$

Refinement

Refinement on F^2

Least-squares matrix: full

$R[F^2 > 2\sigma(F^2)] = 0.031$

$wR(F^2) = 0.073$

$S = 1.14$

1939 reflections

106 parameters

0 restraints

Hydrogen site location: inferred from
neighbouring sites

H-atom parameters constrained

$w = 1/[\sigma^2(F_o^2) + (0.0359P)^2 + 0.2401P]$

where $P = (F_o^2 + 2F_c^2)/3$

$(\Delta/\sigma)_{\max} = 0.001$

$\Delta\rho_{\max} = 0.27$ e Å⁻³

$\Delta\rho_{\min} = -0.22$ e Å⁻³

Special details

Geometry. All esds (except the esd in the dihedral angle between two l.s. planes) are estimated using the full covariance matrix. The cell esds are taken into account individually in the estimation of esds in distances, angles and torsion angles; correlations between esds in cell parameters are only used when they are defined by crystal symmetry. An approximate (isotropic) treatment of cell esds is used for estimating esds involving l.s. planes.

Fractional atomic coordinates and isotropic or equivalent isotropic displacement parameters (\AA^2)

	<i>x</i>	<i>y</i>	<i>z</i>	$U_{\text{iso}}^*/U_{\text{eq}}$
Mn1	0.000000	0.500000	0.000000	0.02622 (11)
N1	0.20857 (19)	0.56497 (13)	-0.09665 (18)	0.0358 (3)
C1	0.3146 (2)	0.62691 (14)	-0.10034 (19)	0.0313 (4)
S1	0.46152 (6)	0.71704 (4)	-0.10505 (6)	0.04157 (14)
N11	0.14907 (18)	0.52888 (12)	0.24007 (16)	0.0306 (3)
C11	0.1329 (2)	0.46441 (15)	0.3576 (2)	0.0333 (4)
H11	0.057240	0.405168	0.340862	0.040*
C12	0.2207 (2)	0.47971 (15)	0.5022 (2)	0.0350 (4)
H12	0.206448	0.431458	0.582080	0.042*
C13	0.3292 (2)	0.56627 (15)	0.5281 (2)	0.0339 (4)
H13	0.391568	0.577949	0.626157	0.041*
C14	0.3466 (2)	0.63626 (14)	0.40992 (19)	0.0295 (3)
C15	0.2556 (2)	0.61299 (14)	0.2685 (2)	0.0316 (3)
H15	0.269345	0.659337	0.186448	0.038*
C16	0.4577 (2)	0.73525 (14)	0.4322 (2)	0.0340 (4)
H16A	0.564073	0.714074	0.494763	0.041*
H16B	0.480824	0.759048	0.332262	0.041*
N12	0.38812 (18)	0.82892 (11)	0.50551 (17)	0.0319 (3)
H12A	0.391635	0.810986	0.604571	0.038*
H12B	0.279589	0.834201	0.463345	0.038*

Atomic displacement parameters (\AA^2)

	U^{11}	U^{22}	U^{33}	U^{12}	U^{13}	U^{23}
Mn1	0.02752 (18)	0.02188 (18)	0.02836 (19)	-0.00181 (13)	0.00218 (13)	0.00086 (13)
N1	0.0343 (8)	0.0370 (8)	0.0371 (8)	-0.0054 (6)	0.0086 (6)	0.0015 (7)
C1	0.0330 (8)	0.0321 (9)	0.0291 (8)	0.0047 (7)	0.0060 (7)	-0.0012 (7)
S1	0.0355 (2)	0.0368 (3)	0.0526 (3)	-0.00815 (19)	0.0079 (2)	-0.0034 (2)
N11	0.0327 (7)	0.0273 (7)	0.0305 (7)	-0.0022 (5)	0.0019 (6)	-0.0013 (5)
C11	0.0362 (9)	0.0276 (8)	0.0361 (9)	-0.0047 (7)	0.0063 (7)	-0.0024 (7)
C12	0.0424 (9)	0.0305 (9)	0.0326 (9)	-0.0020 (7)	0.0074 (7)	0.0022 (7)
C13	0.0396 (9)	0.0322 (9)	0.0291 (8)	0.0000 (7)	0.0039 (7)	-0.0021 (7)
C14	0.0302 (8)	0.0250 (8)	0.0333 (8)	0.0008 (6)	0.0054 (7)	-0.0033 (6)
C15	0.0359 (8)	0.0269 (8)	0.0313 (8)	-0.0010 (7)	0.0038 (7)	0.0012 (6)
C16	0.0348 (9)	0.0281 (9)	0.0389 (9)	-0.0027 (7)	0.0061 (7)	-0.0043 (7)
N12	0.0334 (7)	0.0253 (7)	0.0368 (8)	-0.0023 (6)	0.0048 (6)	-0.0017 (6)

Geometric parameters (\AA , $^\circ$)

Mn1—N1	2.1955 (15)	C12—C13	1.378 (3)
Mn1—N1 ⁱ	2.1955 (15)	C12—H12	0.9500
Mn1—N12 ⁱⁱ	2.2901 (14)	C13—C14	1.388 (2)
Mn1—N12 ⁱⁱⁱ	2.2901 (14)	C13—H13	0.9500
Mn1—N11	2.3154 (14)	C14—C15	1.388 (2)
Mn1—N11 ⁱ	2.3154 (14)	C14—C16	1.509 (2)
N1—C1	1.159 (2)	C15—H15	0.9500
C1—S1	1.6406 (18)	C16—N12	1.483 (2)
N11—C11	1.340 (2)	C16—H16A	0.9900
N11—C15	1.347 (2)	C16—H16B	0.9900
C11—C12	1.385 (3)	N12—H12A	0.9100
C11—H11	0.9500	N12—H12B	0.9100
N1—Mn1—N1 ⁱ	180.0	C13—C12—H12	120.6
N1—Mn1—N12 ⁱⁱ	91.17 (6)	C11—C12—H12	120.6
N1 ⁱ —Mn1—N12 ⁱⁱ	88.83 (6)	C12—C13—C14	119.54 (17)
N1—Mn1—N12 ⁱⁱⁱ	88.83 (6)	C12—C13—H13	120.2
N1 ⁱ —Mn1—N12 ⁱⁱⁱ	91.17 (6)	C14—C13—H13	120.2
N12 ⁱⁱ —Mn1—N12 ⁱⁱⁱ	180.0	C15—C14—C13	117.45 (16)
N1—Mn1—N11	89.18 (5)	C15—C14—C16	120.37 (16)
N1 ⁱ —Mn1—N11	90.82 (5)	C13—C14—C16	122.17 (16)
N12 ⁱⁱ —Mn1—N11	89.52 (5)	N11—C15—C14	124.18 (16)
N12 ⁱⁱⁱ —Mn1—N11	90.48 (5)	N11—C15—H15	117.9
N1—Mn1—N11 ⁱ	90.82 (5)	C14—C15—H15	117.9
N1 ⁱ —Mn1—N11 ⁱ	89.18 (5)	N12—C16—C14	114.17 (14)
N12 ⁱⁱ —Mn1—N11 ⁱ	90.48 (5)	N12—C16—H16A	108.7
N12 ⁱⁱⁱ —Mn1—N11 ⁱ	89.52 (5)	C14—C16—H16A	108.7
N11—Mn1—N11 ⁱ	180.0	N12—C16—H16B	108.7
C1—N1—Mn1	152.67 (14)	C14—C16—H16B	108.7
N1—C1—S1	178.57 (16)	H16A—C16—H16B	107.6
C11—N11—C15	116.67 (15)	C16—N12—Mn1 ^{iv}	120.72 (11)
C11—N11—Mn1	122.20 (11)	C16—N12—H12A	107.1
C15—N11—Mn1	121.12 (11)	Mn1 ^{iv} —N12—H12A	107.1
N11—C11—C12	123.38 (16)	C16—N12—H12B	107.1
N11—C11—H11	118.3	Mn1 ^{iv} —N12—H12B	107.1
C12—C11—H11	118.3	H12A—N12—H12B	106.8
C13—C12—C11	118.75 (17)		

Symmetry codes: (i) $-x, -y+1, -z$; (ii) $x-1/2, -y+3/2, z-1/2$; (iii) $-x+1/2, y-1/2, -z+1/2$; (iv) $-x+1/2, y+1/2, -z+1/2$.

Hydrogen-bond geometry (\AA , $^\circ$)

$D-H\cdots A$	$D-H$	$H\cdots A$	$D\cdots A$	$D-H\cdots A$
C12—H12 \cdots S1 ⁱⁱⁱ	0.95	2.99	3.7264 (19)	136

N12—H12A...S1 ^v	0.91	2.81	3.7016 (16)	166
N12—H12B...S1 ^{vi}	0.91	2.66	3.5224 (15)	159

Symmetry codes: (iii) $-x+1/2, y-1/2, -z+1/2$; (v) $x, y, z+1$; (vi) $x-1/2, -y+3/2, z+1/2$.